Correlation between growth conditions, nanostructural, and morphological characteristics of vanadium pentoxide thin films deposited by low energy plasma focus device

M. GHASEMLOO[a], M. T. HOSSEINNEJAD[b,*], M. ETTEHADI ABARI[b]
aDepartment of Physics, Yadegar-e-Imam Khomeini (RAH) Shahre Rey Branch, Islamic Azad University, Tehran, Iran
bYoung Researchers and Elites Club, Science and Research Branch, Islamic Azad University, Tehran, Iran

Vanadium pentoxide (V_2O_5) thin films were deposited on glass substrates using a low energy (1.3 kJ) plasma focus device. The V_2O_5 thin films were deposited with 10, 20 and 30 shots. The XRD results demonstrated that the degree of crystallinity and the average grain size of the V_2O_5 thin films enhance with more shots. Raman scattering analysis revealed the formation of the V_2O_5 thin films which was in suitable agreement with the XRD results. The SEM and AFM analyzes indicated a growth of nanoparticles/agglomerates on the surface of films, and enhancement of surface roughness of layers with increasing of shots.

1. Introduction

Vanadium oxides make an interesting group of materials such as VO, V_2O_3, VO_2, V_2O_5 and so on, due to their varying oxidation states between V^{2+} and V^{5+} [1]. Among all of these, vanadium pentoxide (V_2O_5), is particularly a interesting material for applications in microelectronics devices [2,3], electronic and optical switches [4], and cathodes for solid-state batteries [5]. In the last years some researchers are synthesized different V_2O_5 forms including nanotubes, nanowires, nanorodes, nanobelts and thin films by various methods such as sol–gel [6], spray pyrolysis [7], magnetron sputtering [8], pulsed laser deposition [9], and thermal decomposition method [10]. In this paper, for the first time we are used plasma focus device for deposition of vanadium oxide thin films and investigated structural and morphological properties of V_2O_5 thin films deposited by this method.

Plasma focus (PF) [11] is a simple pulse plasma device which produces a high temperature (1–2 keV) and high density (10^{25}–10^{26} m^{-3}) plasma column for a short time of 10^{-7} s, using a self-generated magnetic field. This device is an appropriate source of neutrons, soft/hard X-rays, relativistic electrons and energetic ion beams [12-14]. These high energy ions can be utilized for different applications such as surface modification [15], ion implantation [16], thermal surface treatment [17] and thin film deposition [18-20].

The PF device as a source of high energy ions for processing of materials has remarkable advantages such as high deposition rate, energetic deposition process and possible deposition under reactive back-ground gas pressures. It is noticeable that thin films deposited by this method show higher surface quality, with suitable adhesion to the substrate because of its broad ion energy spectrum, grain growth of various compounds through nucleation by successive shots at room temperature environment [21].

These interesting features of the PF device for the thin film deposition, and also recent upsurges in the use of the PF as a potentially suitable candidate for materials processing motivate us to employ it in a somewhat different material processing scheme. The idea is to take superiority of the high energy radiation from plasma focus to deposit V_2O_5 thin films using low energy PF device. The thin films are deposited on to glass substrates at room temperature with various number of focus shots (10, 20 and 30 shots) at constant distance from the tip of anode (10 cm). X-ray diffractometer (XRD) and Raman scattering are used to study the Phase composition of deposited thin films, whereas scanning electron microscopy (SEM) and atomic force microscopy (AFM) are employed to investigate the surface morphology of the thin films.

2. Experimental details

V_2O_5 thin films are deposited onto glass substrate at room temperature by a low energy (1.3 kJ) Mather type PF device. Fig. 1 presents a schematic arrangement of the experimental setup along with the focus subsystem.

As it is shown in Fig. 1, the anode is located at the center and the coaxial electrodes are configured in a twelve copper electrode squirrel cage design for the cathodes. The anode contained of a solid copper rod designed to attach a target at the top end of the anode. As it is observable from Fig. 1, in order to form the V_2O_5 thin films a high purity metallic Vanadium target is mounted in

central hollow copper anode. The technical parameters of PF device for synthesis of V_2O_5 thin films are presented in Table 1.
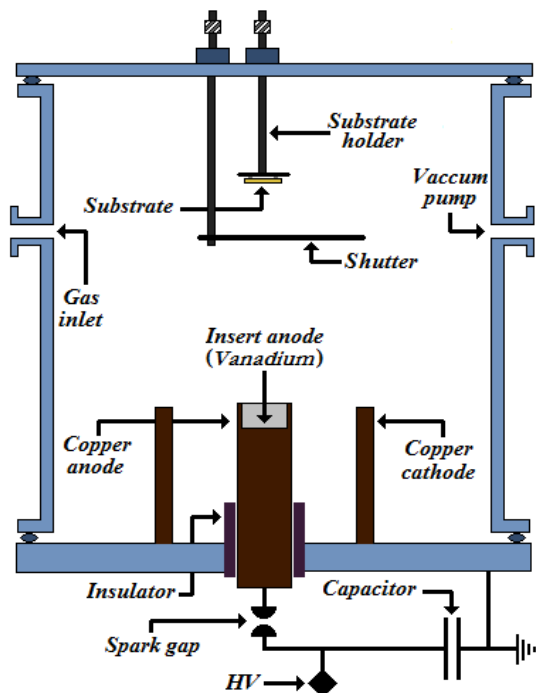
Fig. 1. The schematic of the plasma focus device employed for V_2O_5 thin film deposition

Table 1. The technical parameters of PF device for synthesis of V_2O_5 thin films

Operating parameters	Description
Capacitance	10 µF
Operating charging voltage	16 kV
Stored energy	1.3 kJ
Peak discharge current	130 kA
Inductance of circuit	90 nH
Working gas (Ratio)	Argon:Oxygen (7:3)
Base pressure	10^{-3} torr
Filling gas pressure	1 torr
Substrate temperature	Room temperature (295 K)

The focus chamber is evacuated up to 10^{-3} Torr by a rotary vane pump. After evacuation of chamber, the argon–oxygen admixture is used as a working gas. Our researches on the powerful focusing demonstrated that the best outcome was obtained with the argon:oxygen ratio of 7:3 at a combined filling gas pressure of 1 Torr. Hence, all V_2O_5 thin films are deposited with this combination.

In the current experiment, V_2O_5 thin films are deposited on $10 \times 10 \times 1$ mm^3 glass substrates which are ultrasonically cleaned with alcohol and later acetone, each for a period of 10 min. The substrates are mounted centered onto a substrate holder at the distance of 10 cm from the anode tip. In this study, V_2O_5 thin films are deposited by 10, 20 and 30 shots. A removable shutter is placed between the sample holder and the anode tip. After

obtaining suitable focusing this shutter is removed, and the V_2O_5 thin films are deposited with different number of shots. The degree of focusing action in PF device is indicated by a sharp voltage peak in the voltage probe signal. It is recorded by a four-channel TDS 2014B (100 MHz) TEKTRONIX digital oscilloscope (see Fig. 2).
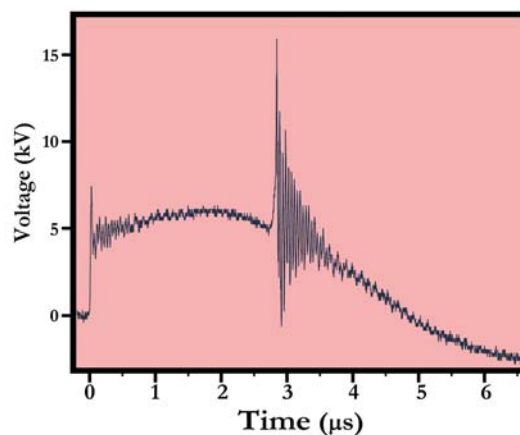
Fig. 2. Voltage signal of a typical plasma focus discharge

The qualitative explanation of the process of formation of V_2O_5 thin film, based on the approximate characteristics of plasma and ion beam in PF device, is as follows: during the radial collapse phase of the plasma focus operation, the temperature of the pinch plasma is so high that it leads to the complete dissociation and ionization of the filling gas species (in this experiment; oxygen and argon). After collapse of plasma column during the radial collapse phase, the electrons and ions accelerate in opposite directions (i.e., towards the anode and towards the substrate), respectively. The bombardment of the substrate by accelerated high energy ions of argon and oxygen, results in a significant and rapid increase in the substrate temperature and modifying the surface without damaging the substrate. Furthermore, the bombardment of the high purity vanadium target mounted in central hollow anode by accelerated relativistic electrons (which moves towards anode tip) ablate the solid vanadium anode tip resulting in the formation of vanadium plasma which react chemically with the reactive oxygen ions of the filling gas species to form V_2O_5 and then deposit on substrate [22].

Phase composition of deposited thin films are investigated using a Philips diffractometer (Xpert pw3373) with CuKα radiation source and by Raman scattering using the JASCO NRS-4100 spectrometer equipped with a laser emitting a wavelength of 457 nm, as an excitation source. Morphological properties of deposited samples are studied by scanning electron microscopy (SEM, Hitachi S-4160) and atomic force microscopy (AFM, Auto Probe Pc; in contact mode, with low stress silicon nitride tip of less than 200 Å radius and tip opening of 18°) analysis. The thickness of deposited V_2O_5 thin films is investigated using surface profiler with the accuracy of 10 nm (Dektak 3030, Veeco Instruments Inc.) and also cross-sectional SEM images.

3. Results and discussion

Fig. 3 shows the XRD patterns of V_2O_5 thin films deposited onto glass substrates at room temperature using different number of shots, at 10 cm axial position from the anode tip and 0° angular position with respect to anode axis. These XRD patterns indicate the successful development of V_2O_5 polycrystalline structures on glass substrates for all deposited samples. From XRD patterns it is observable that the material crystallizes as V_2O_5 orthorhombic phase (space group Pmmn) and the respective positions of the diffraction peaks are matched well with joint committee for powder diffraction standards (JCPDS) standard data for V_2O_5 powders (refer to JCPDS card No. #09-0387).
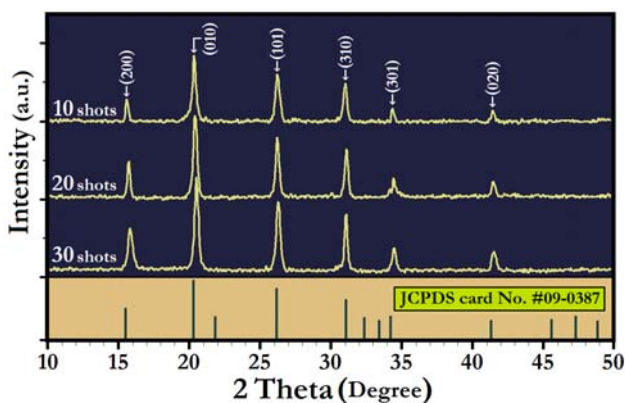
Fig. 3. XRD patterns of the V_2O_5 thin films deposited with different number of shots

XRD patterns also reveal an up-shifting in the positions of V_2O_5 diffraction peaks, from their corresponding stress-free data. It is known that the residual stresses developed in the deposited samples (tensile and compressive stresses) lead to the down and up-shifting in the diffraction peaks from their corresponding stress-free data, respectively. Residual stresses in deposited thin films can be attributed to the creation of point defects (vacancies by knocking off the high energy ions), pulsed thermal shocks due to the intense transient heating of deposited film by high energy ions, and also lattice distortion (strain) [23, 24]. The mentioned strain leads to the change in the d-spacing and hence the displacement of diffraction peaks.

The variation of intensities of V_2O_5 (2 0 0), V_2O_5 (0 1 0), V_2O_5 (1 0 1) and V_2O_5 (3 1 0) diffraction peaks as a function of shots are shown in Fig. 4. From Fig. 4 it is clear that for the thin films deposited with the different number of shots, the peak intensity increases with more shots. This variation in the peak intensities can be clarified in terms of the characteristic features of plasma focus based deposition method and deposition parameters. In particular, in PF device irradiated high energy ions in each shot can lead to rapid increase in the surface temperature which this phenomenon leads to the development of crystallinity.

The average crystallite sizes (D) of V_2O_5 thin films were calculated using the Scherrer formula [25]:

$$D = (0.9\lambda) / (B \cos\theta) \quad (1)$$

where λ is the X-ray wavelength, B is the full width at half maximum (FWHM) of the diffraction peak and θ is the maximum of the Bragg's diffraction angle (in radians).

For the V_2O_5 thin films deposited with 10, 20 and 30 shots, the average crystallite size was estimated to be 16, 27 and 35 nm, respectively. Based on the presented results, the average crystallite size enhances with the increasing of shots. The main reason for this phenomenon can be the enhanced transient and local annealing of the deposited surface layer with the increasing of shots.
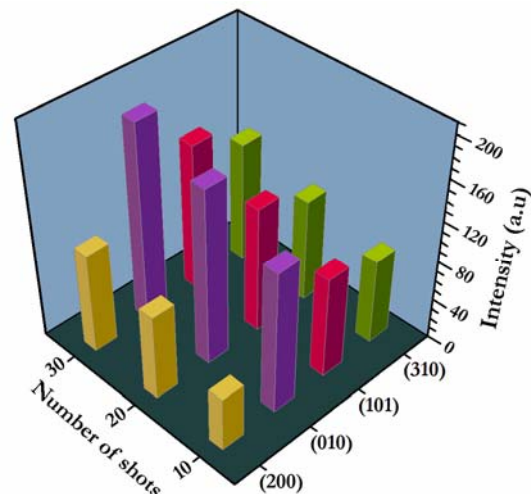
Fig. 4. The variation of intensities of different V_2O_5 diffraction peaks as a function of shots

The Raman spectrum for thin film deposited with 10 shots is presented in Fig. 5. From this spectrum, it is observable that Raman peaks are located at 140, 284, 399, 484, 522, 698 and 994 cm^{-1}. All peaks revealed in this spectrum are related to the typical vibration of crystalline V_2O_5 [26]. The presented results are in suitable agreement with the literature data [26–28] (Table 2).
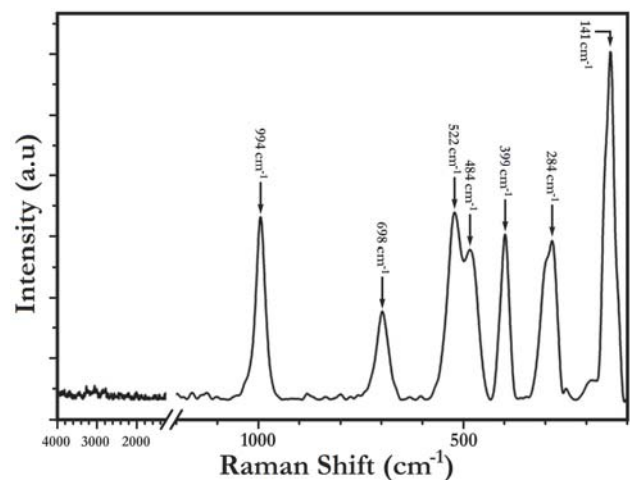
Fig. 5. The Raman spectrum for thin film deposited with 10 shots

Table 2. Comparison of the Raman modes in [cm⁻¹] of V₂O₅ films determined in the present work with the values of other authors

Present research	J.P. Schreckenbach et al. (Electrochem. deposition) [26]	S.H. Lee et al. (RF sputtering) [27]	Q. Su et al. (DC magnetron) [28]
141	143	142	146
284	-	283	286
399	405	405	404
484	-	487	-
522	526	530	520
698	-	706	706
994	983	1000	992

In particular, 141 cm⁻¹, 284 cm⁻¹, 399 cm⁻¹, 484 cm⁻¹, 522 cm⁻¹ and 698 cm⁻¹ frequencies are correspond to V-O-V stretching and bending modes and high frequency peak located at 994 cm⁻¹ is related to the terminal oxygen V=O stretching which results from an unshared oxygen [26-30].

Fig. 6 shows the SEM images of thin films deposited using different number of shots. The SEM micrograph of sample deposited by 10 shots exhibits granular surface and homogeneous distribution of grains on the surface of thin film (see Fig. 6(a)). Thenceforth, by increasing the number of shots (20 and 30 shots), the nucleated structures on a nanometer scale are developed (see Fig. 6 (b) and (c)). The growth of nanostructures can be due to more energy being transferred to the sample by increasing of shots, leading to a higher mobility of nanoparticles and hence resulting in the larger sized agglomerates.
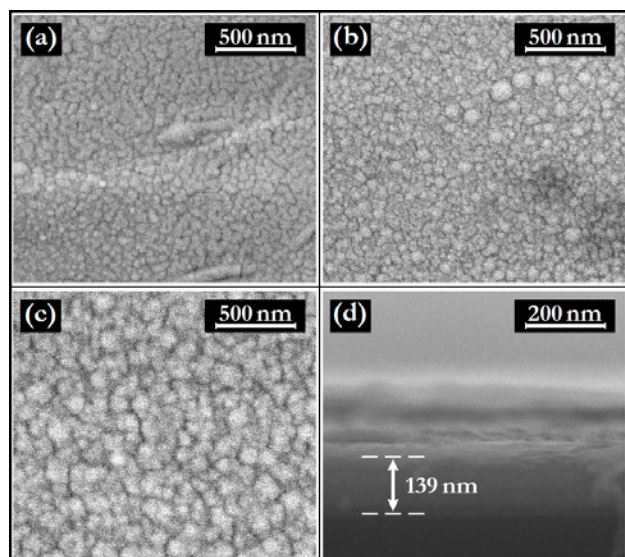
Fig. 6. SEM images of V₂O₅ thin films deposited by different number of shots: (a) 10 shots (b) 20 shots (c) 30 shots and (d) cross-sectional SEM view of thin film deposited by 10 shots

Table 3 presents the average thickness of the V₂O₅ thin films estimated by a surface profiler with the accuracy of 10 nm (Dektak 3030, Veeco instruments Inc.). The results presented in table 3 indicate that thickness of the

deposited thin films enhances with increasing the number of shots from 10 to 30 shots. This correlation is in strong agreement with the results obtained from XRD analysis. Fig. 6d illustrates the typical cross-sectional SEM image of thin film deposited using 10 shots, demonstrating great consistency between the thickness of V₂O₅ thin film deposited with 10 shots and that obtained from the surface profiler.

We investigated the surface morphology of the deposited thin films using AFM analysis. Fig. 7 presents the 2D and 3D images of surface topography of the V₂O₅ thin films deposited with different number of shots. In this analysis, all the images were obtained with a scanning area of 3 μm × 3 μm. The AFM images illustrate that the grains/clusters grow on the surface of deposited samples with more shots. The increasing of size of grains/clusters with the enhancement of shots can be explained by the increased transient and local annealing of the deposited surface layer. Indeed, with increasing of the energetic ions irradiation, more energy is transferred to the film surface, leading to greater mobility of nanoparticles, hence resulting in bigger sized grains/clusters. This scrutiny also reveals the crucial role of the total energy deposited by energetic ions on surface morphological properties of the thin film.
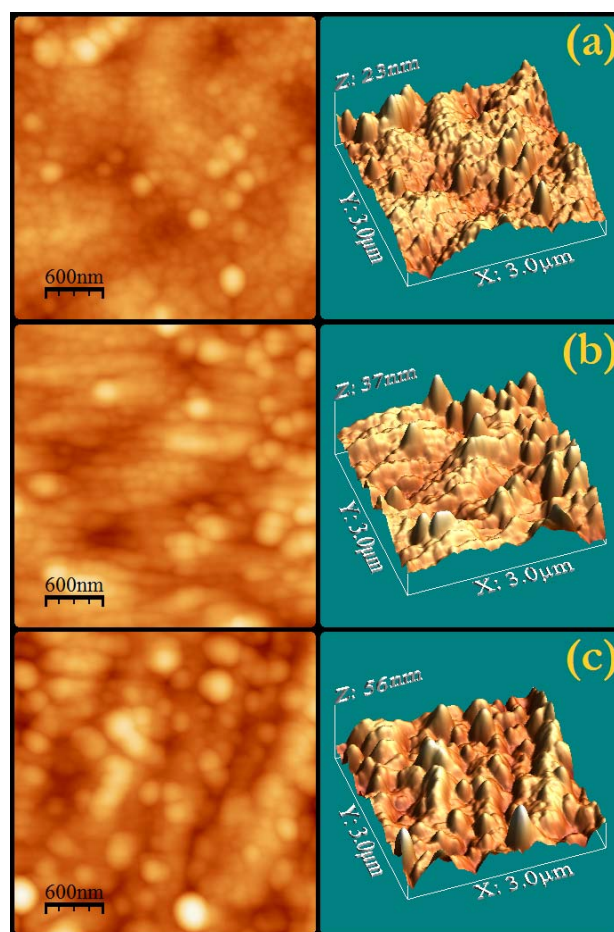
Fig. 7. AFM micrographs of the V₂O₅ thin films deposited with (a) 10 shots (b) 20 shots and (c) 30 shots

Fig. 8 presents the histograms of grain sizes on the surface of the V_2O_5 thin films deposited with different numbers of shots. The results indicate that for samples deposited with more shots, the distributions of the grains on the sample surfaces become more heterogeneous. The patterns given in Fig. 8 also illustrate a rise in the size of most of the grains with increasing the number of shots from 10 to 30 shots. This growth in the size of most of the grains can be attributed to the increase in the strength of the annealed deposited thin film with increasing of shots.
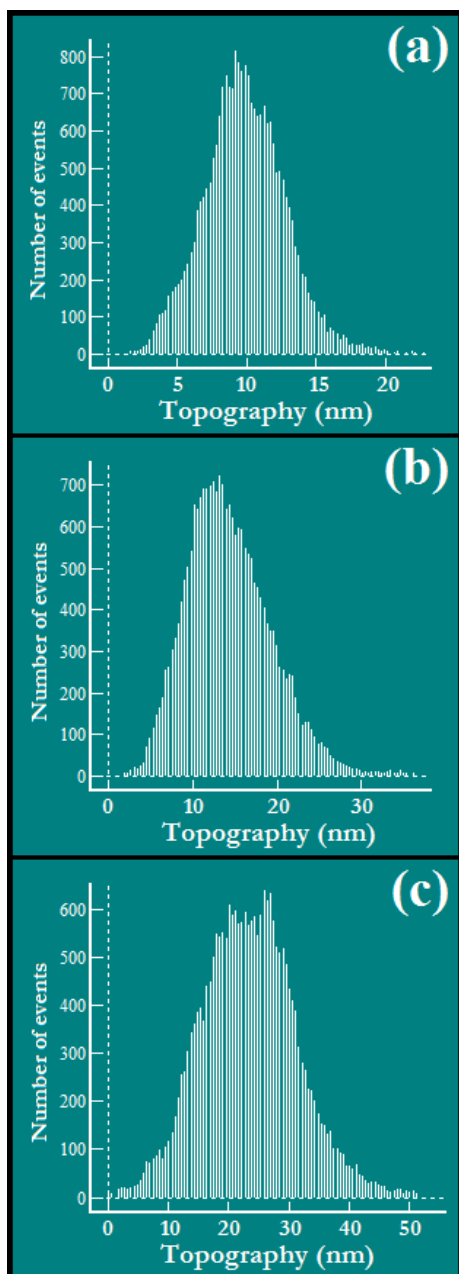
Fig. 8. Histograms of distribution of size of grains on the surface of the V_2O_5 thin films deposited with (a) 10 shots (b) 20 shots and (c) 30 shots

In order to further investigation of histograms of grain sizes, we fitted the Gaussian curves to the histograms. The full width at half maximum (FWHM) of fitting Gaussian curves to the histograms are listed in table 3. The results presented in Table 3 reveal smaller FWHM values (narrower distributions with sharper peaks) with fewer shots. Therefore, the grains are more homogeneously distributed on the surface of the thin films deposited with fewer shots.

Table 3. The average thickness of V_2O_5 deposited thin films and FWHM of the Gaussian curves fitted on the histograms of distribution of grain sizes

Number of Shots	average thickness (nm)	FWHM (nm)
10	140	8
20	260	11
30	370	19

Larger active surface is an important factor in fabrication of many devices such as light and gas sensors. The active surface is proportional to surface roughness parameters such as roughness exponent, correlation length, and standard deviation [31]. In this study, to investigate and compare the surface roughness of the deposited samples, we measured the roughness of three random areas over the surface of the deposited film and recorded the average and root mean square (rms) values of the roughness measurements. The rationale behind this is that, in plasma focus the ions are radiated in a fountain-like structure, and their energy and flux varies with their angle relative to the anode axis [32]. Thus, different areas of the film surface are expected to have different roughness. This variety is taken into consideration by picking random areas and computing the average and rms of their roughness. The measured average and rms roughness values for samples deposited with different number of shots are shown in Fig. 9.
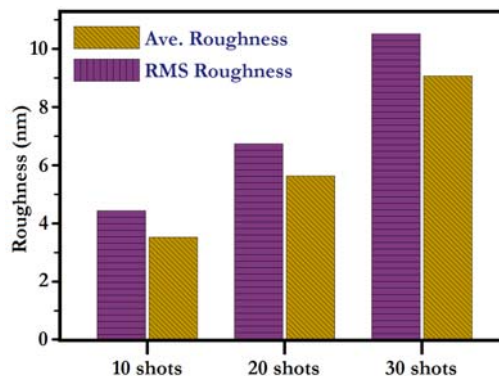
Fig. 9. The variations of the RMS and average roughness of the V_2O_5 thin films as a function of shots

The results presented in Fig. 9 show an increase in the surface roughness when the number of shots is enhanced from 10 to 20 and then 30 shots. This increase was predictable because the larger number of shots leads to the bombardment of sample surfaces with higher energy ions, and as a result the deposited coating becomes coarser. In addition, as previously mentioned, with increasing the

shots, the size of the surface grains becomes larger, and therefore roughness of the deposited thin films increases.

4. Conclusions

This study presents an effective procedure to plasma-based nanofabrication, via energetic ions emitted after collapse of plasma column during the radial collapse phase of plasma focus discharge. A systematic research has been carried out to investigate the effect of the different number of shots (10, 20 and 30 shots) in the PF treatment, on the growth behavior of V_2O_5 phase on the glass substrate.

XRD spectra indicated that the degree of crystallinity and the average grain size of the V_2O_5 thin films enhance with increasing the number of shots. The results obtained from Raman scattering analysis revealed the formation of the V_2O_5 thin films which was in suitable agreement with the XRD results. From AFM results a significant rise was observed for the sizes of the nanostructures and the size of most of the grains formed on the surface of the deposited samples. Moreover, both average and rms surface roughness of the thin films enhanced as they were exposed to more shots. The results presented in this work indicate that using a plasma focus device can be the method of choice with many potential applications in preparation of thin oxide layers.

In this research, we focused on investigating the variations of different properties with the number of shots only, and in all experiments, the film was positioned in a constant distance (10 cm) from the anode tip and 0° angular position with respect to anode axis. In a possible extension of this experiment, the effect of the distance of the substrate from the anode tip (with the same number of shots) can be scrutinized. Another extension for future research is to investigate thin films deposited at different angular positions with respect to anode axis.

References

[1] I. Mjejri, A. Rougier, M. Gaudon, Inorg. Chem. **56**, 1734 (2017).

[2] Z. Wan, R.B. Darling, M.P. Anantram, Phys. Chem. Chem. Phys. **17**, 30248 (2015).

[3] S. Beke, Thin Solid Films **519**, 1761 (2011).

[4] A. Dhawan, Y. Sharma, L. Brickson, J.F. Muth, Optical Materials Express **4**, 1128 (2014).

[5] C. F. Armera, M. Lubkeb, M. V. Reddyd, J. A. Darrc, X. Lib, A. Lowe, Journal of Power Sources **353**, 40 (2017).

[6] V. Modafferi, G. Panzera, A. Donato, P. L. Antonucci, C. Cannilla, N. Donato, D. Spadaro, G. Neri, Sens. Actuators B **163**, 61 (2012).

[7] A. A. Mane, V. V. Ganbavle, M. A. Gaikwad, S. S. Nikam, K. Y. Rajpure, A. V. Moholkar, Journal of Analytical and Applied Pyrolysis **115**, 57 (2015).

[8] W. Yan, M. Hu, D. Wang, C. Li, Appl. Surf. Sci. **346**, 216 (2015).

[9] J. Huotari, R. Bjorklund, J. Lappalainen, A. Lloyd Spetz, Sens. Actuators B **217**, 22 (2015).

[10] R. Suresh, K. Giribabu, R. Manigandan, S. Praveen Kumar, S. Munusamy, S. Muthamizh, A. Stephen, V. Narayanan, Sens. Actuators B **202**, 440 (2014).

[11] J. W. Mather, Methods Exp. Phys. **9**, 187 (1971).

[12] Sh. Al-Hawat, S. Saloum, Contrib. Plasma Phys. **49**, 4 (2009).

[13] Sh. Al-Hawat, M. Akel, S. Lee, H. Saw, J. Fusion Energy **31**, 13 (2012).

[14] Sh. Al-Hawat, M. Akel, S. Shaaban, J. Fusion. Energy **34**, 163 (2015).

[15] Z. A. Umar, R. S. Rawat, R. Ahmad, Z. Chen, Z. Zhang, J. Siddiqui, A. Hussnain, T. Hussain, M. A. Baig, Surf. Interface Anal. **49**, 548 (2017).

[16] S. K. Ngoi, S. L. Yap, B. T. Goh, R. Ritikos, S. A. Rahman, C. S. Wong, J. Fusion Energy **31**, 96 (2012).

[17] I. A. Khan, R. S. Rawat, R. Ahmad, M. A. K. Shahid, Appl. Surf. Sci. **288**, 304 (2014).

[18] Z. A. Umar, R. S. Rawat, K. S. Tan, A. K. Kumar, R. Ahmad, T. Hussain, C. Kloc, Z. Chen, L. Shen, Z. Zhang, Nucl. Instrum. Methods Phys. Res. B **301**, 53 (2013).

[19] M. Ahmad, Sh. Al-Hawat, M. Akel, O. Mrad, J. Appl. Phys. **117**, 063301 (2015).

[20] M. J. Inestrosa-Izurieta, P. Jauregui, L. Soto, J. Phys.: Conf. Ser. **720**, 012045 (2016).

[21] R. S. Rawat, V. Aggarwal, M. Hassan, P. Lee, S. V. Springham, T. L. Tan, S. Lee, Appl. Surf. Sci. **255**, 2932 (2008).

[22] R. S. Rawat, Nanosci. Nanotech. Lett. **4**, 251 (2012).

[23] V. N. Gurarie, P. H. Otsuka, D. N. Jamieson, S. Prawer, Nucl. Instrum. Methods Phys. Res. B, **242**, 421 (2006).

[24] M. Shirazi, M. Ghasemloo, G. R. Etaati, M. T. Hosseinnejad, M. R.Toroghinejad, J. Alloy. Comp. **727**, 978 (2017).

[25] B. D. Cullity, S. R. Stock, Elements of X-ray diffraction, vol. 3, Prentice Hall, New-Jersey, 2001.

[26] J. P. Schreckenbach, K. Witke, D. Butte, G. Marx, Fresenius J. Appl. Chem. **363**, 211 (1999).

[27] S. H. Lee, H. M. Cheong, M. J. Seong, P. Liu, C. E. Tracy, A. Mascarenhas, J. Appl. Phys. **92**, 1893 (2002).

[28] Q. Su, Q. Liu, M. L. Ma, Y. P. Guo, Y. Y. Wang, J. Solid State Electrochem. **12**, 919 (2008).

[29] A. Gornstein, A. Khelfa, J. P. Guesdon, C. Julien, Mater. Res. Soc. Symp. Proc. **369**, 649 (1995).

[30] C. Julien, GA. Nazri, O. Bergstrom, Phys. Status Solidi (b) **201**, 319 (1997).

[31] G. R. Jafari, M. R. Rahimi Tabar, A. Irajizad, G. Kavei, Phys. A **375**, 239 (2007).

[32] L. Bertalot, H. Herold, U. Jager, A. Mozer, T. Oppenlander, M. Sadowski, H. Schmidt, Phys. Lett. A **79**, 389 (1980).

*Corresponding author: hoseinnejad.pprc@gmail.com